NUKLEONIKA 2012;57(2):257–263

ORIGINAL PAPER

Non-homogeneities in multi-element plasmas

Ewa Pawelec

Abstract. This work presents the results of modeling and measurements of plasma parameters performed in a wall--stabilized arc working in a mixture of gases. The temperature and composition of the plasma are analyzed and the homogeneity of the plasma along the arc column in different gas mixtures is studied.

Key words: plasma spectroscopy • wall-stabilized arc • demixing in plasma • plasma modeling

E. Pawelec
Institute of Physics,
University of Opole,
48 Oleska Str., 45-052 Opole, Poland,
Tel.: +48 77 452 7286, Fax: +48 77 452 7290,
E-mail: ewap@uni.opole.pl

Received: 5 October 2011
Accepted: 25 November 2011

Introduction

Wall-stabilized atmospheric pressure arcs working in a mixture of gases are standard sources for many types of applications. One of their most prominent applications in basic research is the measurement of atomic and ionic parameters, including transition probabilities [6], Stark widths and shifts [1]. Wall-stabilized arcs are widely used for those measurements, because of their stability, homogeneity of the plasma and possibility of obtaining plasma in conditions close to thermal equilibrium. Plasmas in wall-stabilized arcs can also have very different electron densities, depending on the plasma composition and this feature is very useful for measurement of line-broadening parameters which depend on the electron density (Stark widths, shifts and asymmetry).

Measurements in the wall-stabilized arc are often performed in a mixture of gases, along or across the arc axis (end-on and side-on measurement geometry). This work presents studies of the uniformity of the plasma parameters in a multi-element plasma (in this case created in mixtures of argon and one other atomic or molecular gas), performed both by modeling of the plasma and by optical emission spectroscopy measurements.

Plasma modeling

Modeling of atmospheric pressure arc plasmas is performed mainly using the sets of magnetohydrodynamic equations. In the case of the one-element plasma those equations are as follows [7]:

– mass conservation

$$\frac{\partial \rho}{\partial t} + \nabla \cdot (\rho \vec{v}) = 0 \quad (1)$$

– momentum conservation

$$\rho \frac{\partial \vec{v}}{\partial t} + (\rho \vec{v} \cdot \nabla)\vec{v} = -\nabla p + \nabla \cdot \vec{\tau} + \rho \vec{g} + \vec{j} \times \vec{B} \quad (2)$$

– energy conservation

$$\frac{\partial \rho h}{\partial t} + \nabla \cdot (\rho \vec{v} h) = \vec{j} \cdot \vec{E} - U_{\mathrm{rad}} + \nabla \cdot \left(\frac{\kappa}{c_p} \nabla h \right) + \frac{5k}{2ec_p} \vec{j} \cdot \nabla h \quad (3)$$

– continuity equations, e.g. of the arc current:

$$\nabla \cdot \vec{j} = 0 \quad (4)$$

– Maxwell equations, e.g. for the magnetic field generated by arc current:

$$\nabla \times \vec{B} = \mu_0 \vec{j} \quad (5)$$

– Ohm's law

$$\sigma \vec{E} = \vec{j} \quad (6)$$

In these equations ρ denotes the plasma density; ν – velocity; p – pressure; τ – stress tensor; h – enthalpy; U_{rad} – energy loss from the plasma due to radiation; κ and c_p are the thermal conductivity and specific heat, respectively and σ is the plasma conductivity.

Wall-stabilized arc is a stable plasma source, so all the time derivatives in previous equations can be neglected, and the stable solution can be obtained.

Boundary conditions for wall-stabilized arc have to reflect the experimental arrangement: very weak flow of the input gases into the arc, existence of electrodes on both ends of the plasma column, and two distinctly different regions along the arc – the channel region, which is located inside arc segments and is restricted by water-cooled copper wall a few millimeters from the arc axis and the spacer region, located between arc segments, where plasma expansion is nearly completely unrestricted in the radial direction. Transition from one to the other of these regions is smooth and there are several of them along the arc, so most of the plasma in the wall-stabilized arc is in one of those two regions. The wall-stabilized arc can be described as an axially symmetric plasma source (if the electrodes are located in such a way that they do not disturb the symmetry) so the calculations described above can be performed using only two dimensions in the cylindrical system of coordinates with z along the arc axis and r in the perpendicular direction, as the plasma conditions do not depend on the angle φ. The Eqs. (1–6) can be solved using either enthalpy or temperature as the independent variable, but the temperature is more useful for the comparison with experiment.

Results of calculations for the temperature and velocity in argon arc are shown in Fig. 1. The results are

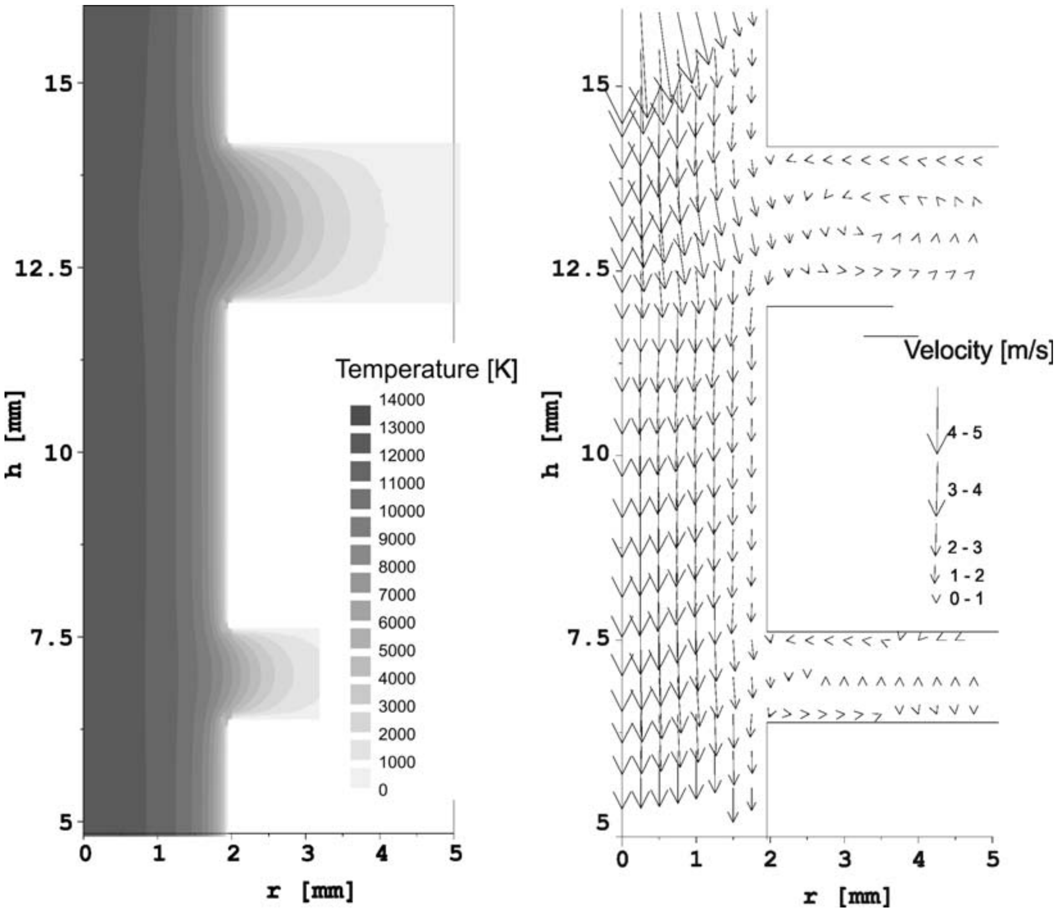

Fig. 1. Model results of spatial distribution of temperature and velocity inside a wall-stabilized arc working in pure argon (arc current – 40 A, arc diameter – 4 mm).

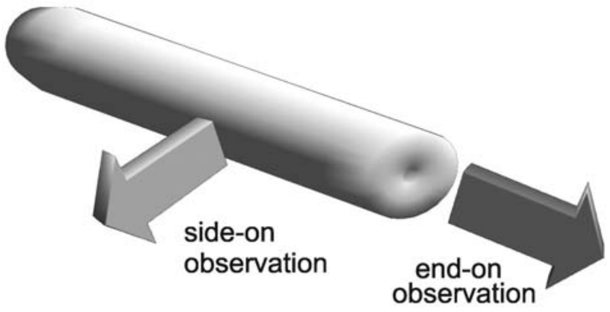

Fig. 2. Possible observation geometries.

different for different working gas composition because transport and thermal coefficients: plasma density, enthalpy, thermal and electrical conductivity, viscosity and so on depend on both temperature and composition of the plasma. Knowledge of those coefficients is essential for any plasma modeling by hydrodynamic equations as described. Unfortunately, there are nearly no experimental verification of such coefficients, they are mostly calculated using many assumptions on the plasma state (mostly either LTE or similar). The situation is even more difficult in the case of multi-element plasmas.

Plasma in a wall-stabilized arc is mostly observed either in the end-on or side-on geometry (Fig. 2). Side-on observations can be performed only in the spacer regions, and they are mostly affixed to the center of the spacer region. End-on observations are performed cross-regions, so the resulting spectra are determined both by the channel and the spacer regions. Figure 3 shows the dependence of the temperature on the position along the observation axis for both end-on and side-on geometry. These curves show that the assumed homogeneity of the plasma along the arc axis is pretty good for the arc center, even better for the regions around $r = 1$ mm and increasingly worse closer to the arc walls. The non-homogeneities along the arc axis depend of course on the spacer thickness. The 2 mm spacer thickness reflected by the length of the gap shown in Fig. 1 may be considered too large (most of the spacers in the experimental arcs are of the order of 1 mm or less), but the segment boundary in the model is very sharp, with exactly 90 degrees angle between the walls. In reality, segments are never as sharp and even if they are, they do not stay that way long, they are eroded to much more rounded shape. The rounded shape of the real segment is therefore better approximated by the larger spacer/gap thickness than by the 1 mm spacer with the sharp edge. Calculations of the proper shape of the segment angle are of course possible, but they would greatly complicate the calculations and increase the calculation time.

Modeling the plasma in a mixture of gases one has to take into account both the magnetohydrodynamic equations (with appropriate corrections) and a set of equations describing diffusion in the plasma. Diffusion in the plasma can be described using the equations for mass fluxes of all q of the plasma components [5]:

$$J_i \equiv m_i n_i v_i = \frac{n^2}{\rho} m_i \sum_{j=1}^{q} m_j D_{ij} d_j - D_i^T \nabla \ln T \tag{7}$$

where i denotes the plasma components. The velocity v_i is relative to the mass-average velocity and D are the diffusion coefficients. The driving force term d describes all the forces driving the diffusion, as the mole gradients, gradients in the total pressure and external forces (as the external electric field). There are q^2 ordinary diffusion coefficients D_{ij} of which $q(q-1)/2$ are linearly independent and q thermal diffusion coefficients of which linearly independent are $(q-1)$.

The amount of species in an arc plasma is very high. In Ar-N_2 mixtures, even if the temperature is rather low (below 1.5 eV) species considered in the plasma have to include Ar, Ar^+, N, N^+, N_2, N_2^+ and electrons, which means $q = 7$ already. There are many methods used to simplify the analysis, one of them is combining the species into the parent gases, described e.g. in [5]. The simplified equation for the mass flux of gas A vs. gas B in the two-gas plasma can be therefore written as (the equation shows the explicit form of the driving term d):

$$\overline{\vec{J}_A} \equiv \frac{n^2}{\rho} \overline{m_A}\,\overline{m_B} (\overline{D_{AB}^x} \nabla \overline{x_B} + \overline{D_{AB}^x}\,\overline{\vec{E}}) - (\overline{D_{AB}^{T1}} + \overline{D_A^T}) \nabla \ln T \tag{8}$$

Bars over the parameters denote that they are describing the gas, not the plasma species; $\overline{m_A}$ is the average mass of the heavy species of gas A; $\overline{x_B}$ is the sum of the mole fractions of all species of gas B. Combined diffusion coefficients D_{AB}^x and others can be found in the publications of Murphy (e.g. [4] for Ar + He mixture) or directly from the present author.

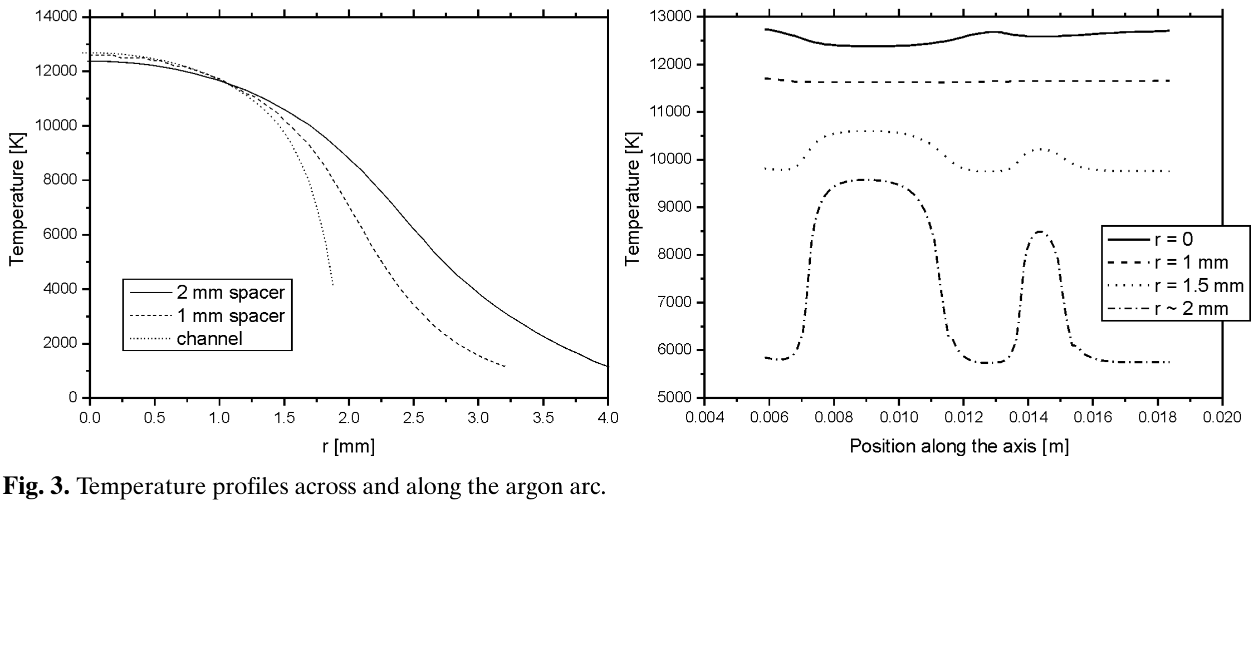

Fig. 3. Temperature profiles across and along the argon arc.

The modified magnetohydrodynamic equation which has to be taken into account in the gas mixture are the energy conservation equation:

$$\text{(9)}\quad \frac{\partial \rho h}{\partial t} + \nabla\cdot(\rho\vec{v}h) = \vec{j}\cdot\vec{E} - U_{\mathrm{rad}} + \nabla\cdot\left(\frac{\kappa}{c_p}\nabla h\right) + \frac{5k}{2ec_p}\vec{j}\cdot\nabla h + \nabla\cdot\left[(\overline{h_A}-\overline{h_B})\left(\overline{\vec{J}_A} - \frac{\kappa}{c_p}\nabla\overline{Y_A}\right)\right]$$

where $\overline{Y_A}$ is the mass fraction of the gas A in the overall mixture.

Calculations of the plasma parameters in the gas mixtures are more complicated than in monospecies gases. Due to the computer and code constraints, only the one-dimensional (1-D) calculations were performed and are presented here. The approximations leading to one-dimensional and *quasi*-two-dimensional (2-D) calculations were as follows:

- Any differences of pressure in the arc are negligible.
- In the channel region and in the center of the spacer region there are no axial gradients of the plasma parameters, so the driving terms apart from the electric field are only in the radial direction.
- In the channel region and in the center of the spacer region the electric field is only in the axial direction, there is no radial electric field.
- Velocity in the arc is negligible, and therefore the mass fluxes are also negligible.

These assumptions lead to two different approximations, one in the radial one in the axial directions. In the radial direction the cataphoresis is neglected and the temperature and plasma composition are calculated using the *quasi*-two-dimensional approximation using the following approximate equations:

$$\text{(10)}\quad \nabla\overline{x_B} = -\nabla\overline{x_A} = \frac{\rho}{n^2}\frac{(\overline{D^{T1}_{AB}}+\overline{D^{T}_{A}})\nabla\ln T}{\overline{m_A}\,\overline{m_B}\,\overline{D^{x}_{AB}}}$$

$$\text{(11)}\quad 0 = \vec{j}\cdot\vec{E} - U_{\mathrm{rad}} + \nabla\cdot\left(\frac{\kappa}{c_p}\nabla h\right) + \frac{5k}{2ec_p}\vec{j}\cdot\nabla h - \nabla\cdot\left[(\overline{h_A}-\overline{h_B})\left(\frac{\kappa}{c_p}\nabla\overline{Y_A}\right)\right]$$

In the axial direction temperature is assumed to be nearly constant and the only driving term in Eq. (8) is the electric field. This calculation was performed only for the Ar + He mixture, as any of the cataphoresis effects are visible only in the mixtures with strong amount of helium. In this case spatial distribution of plasma temperature is taken from radial calculations and the plasma composition along arc axis is calculated using the following equation:

$$\text{(12)}\quad \nabla\overline{x_B} = -\nabla\overline{x_A} = \frac{\rho}{n^2}\frac{\overline{D^{E}_{AB}}\vec{E}}{\overline{m_A}\,\overline{m_B}\,\overline{D^{x}_{AB}}}$$

Results for different plasma compositions are shown in Figs. 4 to 6. The radial distributions of plasma temperatures in the mixtures of argon and one other gas tend to change within a similar way – when the amount of the other gas grows, the temperature lowers in the

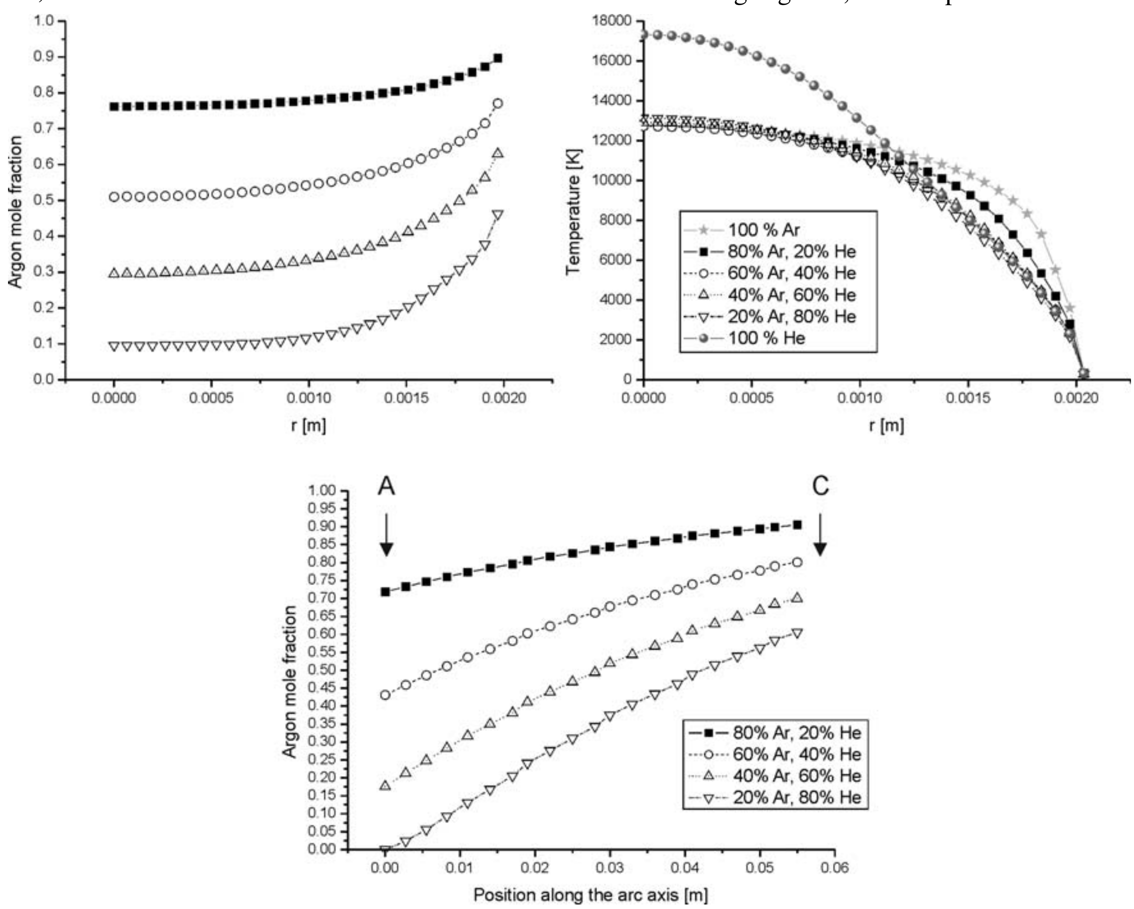

Fig. 4. Radial and axial distribution of plasma parameters in Ar-He mixtures.

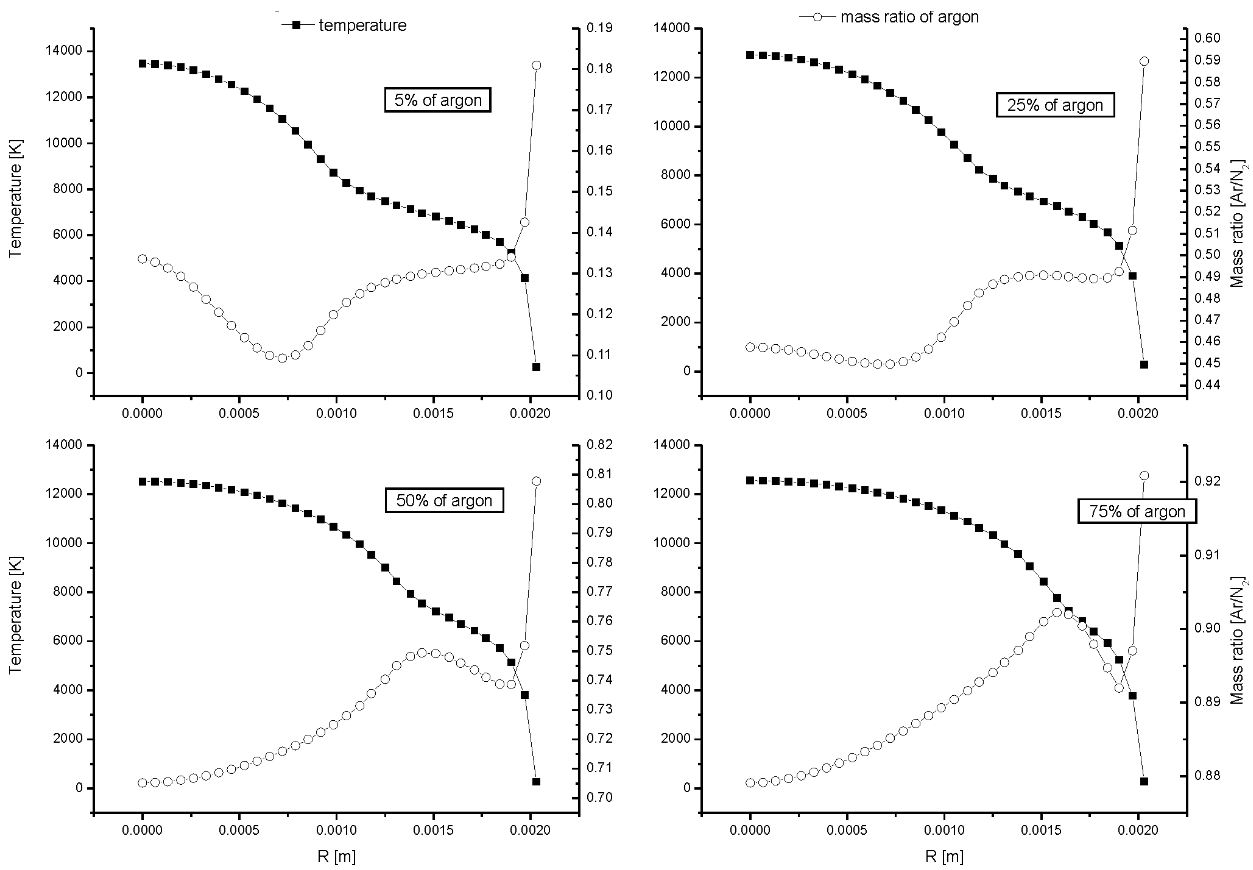

Fig. 5. Radial distribution of plasma parameters in Ar-N_2 mixtures.

outer region of the arc and rises in the arc center. It is much more visible in the case of molecular gases, because in their case the outer regions of the arc are the regions where dissociation of molecular gas is happening. Dissociation requires a large amount of energy which in the case of atomic gas would go into heating the gas, so temperature in this region drops significantly. To keep the same arc current the temperature in the center of the arc has to be higher, to reach the regions of higher conductivity. The temperature distributions in the argon-helium mixtures are very similar to the distribution in pure argon, because the temperature dependence of transport parameters in any helium mixture are dominated by the properties of the admixtures (because the transport parameters depend strongly on the electron density and even in the helium mixture containing 1% of admixtures nearly all electrons are supplied by ionization of the admixture, not of helium).

The strongest feature of the radial distributions of plasma composition is that the heavier gas (argon) is pushed out of the arc center. More subtle features are visible if the mixture includes some molecular gas, where the additional maxima and minima are located close to the sharper gradients in the temperature distributions (Fig. 5). In the argon-nitrogen mixture there

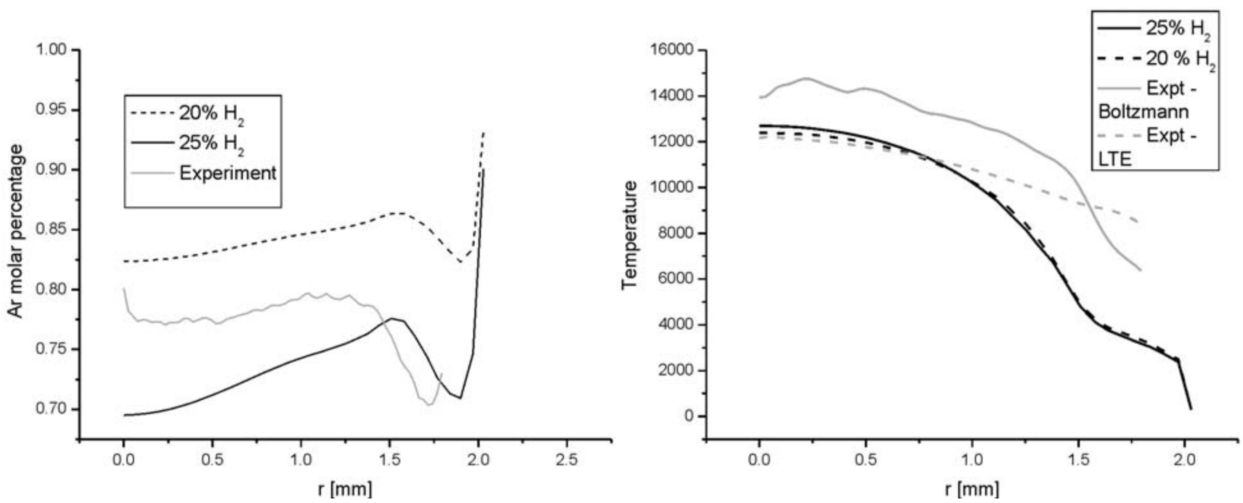

Fig. 6. Radial distribution of plasma parameters in Ar-H_2 mixtures – model and experimental results.

is an additional characteristic feature in the case of low argon content – the distribution of argon mass ratio exhibits a local maximum in the center of the arc.

Experiment

Experiments were performed mostly in side-on observation geometry for three gas mixtures – argon-helium, argon-nitrogen and argon-hydrogen. For argon-nitrogen mixtures, measurements were performed additionally in the end-on geometry. The side-on measurements are more reliable for verification of the plasma parameters, because their analysis leading to local values of plasma parameters needs only the assumption of the axial symmetry. Obtaining local values of plasma parameters from end-on measurements requires assumption of longitudinal homogeneity, which was one of the features of the arc to be to verified, not assumed, in this experiment. Both the arc and the experiment configuration were similar to those described in Ref. [3].

The plasma diagnostics was performed using the emission coefficients of different atomic lines from all the plasma constituent gases, parameters of the line profiles from argon and hydrogen lines and emission coefficients of the rotational components of the molecular band of N_2^+. The atmospheric pressure wall-stabilized arcs are rarely airtight, and the working gases still have some admixtures in them, so lines and bands of nitrogen and hydrogen are visible in most experiments even if those gases were not deliberately added to the working gas. N_2^+ in the arc is mostly produced by the charge exchange, so the population distribution of vibrational levels probably is not very close to the local thermal equilibrium, but the population distribution among rotational levels fits well the Boltzmann distribution. Rotational temperature of molecules in atmospheric pressure plasma is assumed to be equal to the heavy species temperature.

There were several different methods used for calculation of the plasma parameters from measured quantities. Most of them used either the assumptions of at least partial local thermal equilibrium in the plasma. They were as follows:

- Local thermal equilibrium relations (Boltzmann distribution for populations of atomic levels, Saha and Dalton law for populations of atoms and ions) were used to calculate temperature, electron density and plasma composition from absolute emission coefficients of atomic lines.
- Local thermal equilibrium relations (Boltzmann distribution for populations of atomic levels, Saha and Dalton law for populations of atoms and ions) and relations linking Stark widths of atomic lines to electron density and temperature, were used to calculate temperature, electron density and plasma composition from relative emission coefficients of atomic lines and from the Stark broadening of atomic lines (argon lines, H_α or H_β in different experiments).
- Boltzmann distribution for excited atomic levels was used to calculate excitation temperature from relative emission coefficients of the lines originating from the same element (mostly Ar I lines, but also N I).
- Boltzmann distribution of rotational sublevels of the molecular vibrational level was used to calculate rotational temperature from relative emission coefficients of resolved rotational lines in the molecular band 0–0 of the first negative nitrogen system.

The application of the first and second diagnostic methods requires LTE conditions in the plasma, while in the case of remaining methods only partial LTE conditions are required. Unfortunately, obtaining the plasma composition without the LTE assumptions is in multi-element plasmas rather difficult, because it increases significantly the number of plasma parameters (even if only the overpopulation of the ground states of atoms are taken into account), so nearly all the plasma compositions are derived from LTE calculations. Only in the case of argon-helium plasma the overpopulation of the helium ground level was taken into account.

Results and comparison

The results are shown in Figs. 6 to 8. Comparison between the theoretical and experimental curves for temperatures show that the temperatures derived by methods assuming LTE, much better agree with model values of temperatures on the plasma axis, and temperature distributions obtained by using Boltzmann diagram are consistently too high, nevertheless, the temperature distributions obtained using the Boltzmann diagrams reproduce much better the theoretical temperature curves. There are a few different possible explanations for these discrepancies. The temperature from the theo-

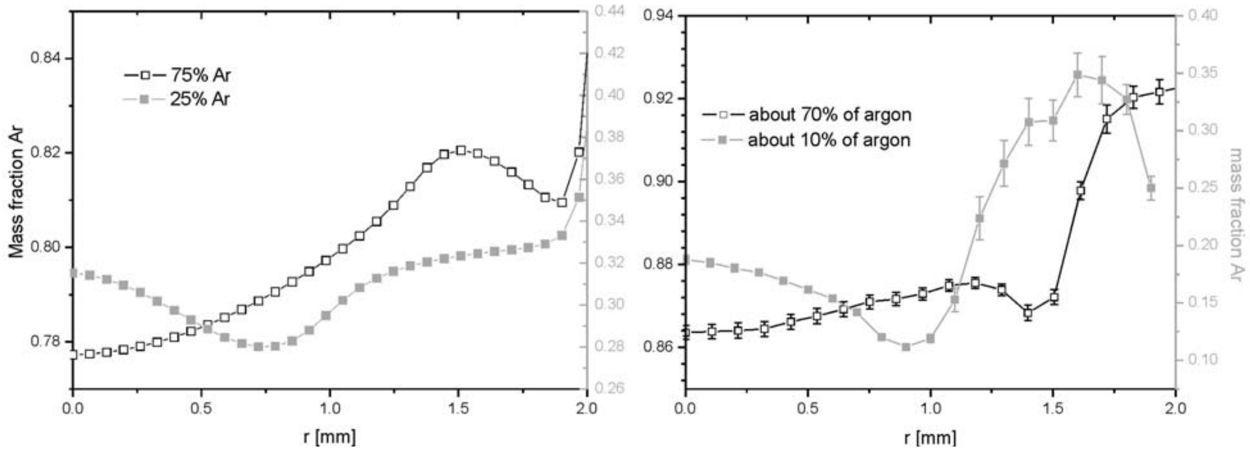

Fig. 7. Radial distribution of plasma parameters in Ar-N_2 mixtures – model (left) and experimental results (right).

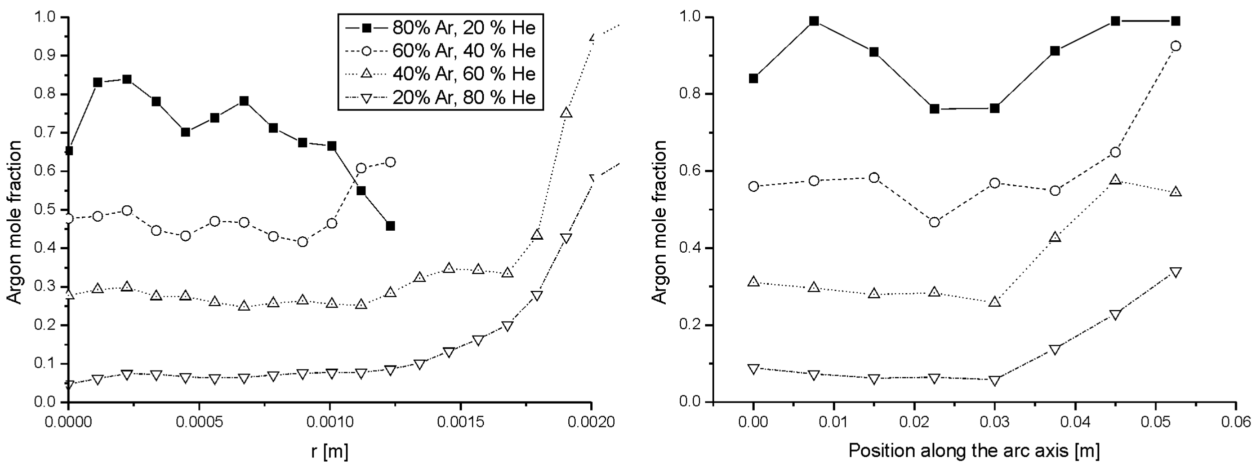

Fig. 8. Radial and axial distributions of plasma composition in Ar-He mixtures.

retical model depends on the quality of the transport coefficients, which adds a significant uncertainty to the results of the modeling. The uncertainties of temperatures calculated from experimental values depend strongly on possible departures from LTE and on the quality of the atomic constants used to calculate populations of the atomic levels from the emission coefficients of the atomic lines. In the case for highly excited argon lines strong enough to be used for the Boltzmann plot the uncertainties of transition probabilities can easily be of the order of 30%.

The results show best agreement in the case of an argon-hydrogen mixture, possibly because equilibrium in such plasma is closest to LTE. Works of Wujec [8] show, that the admixtures of hydrogen greatly improve the equilibrium conditions of an argon arc. This is not the case of nitrogen, but still the qualitative agreement between the experimental and modeled results exist, up to the appearance of the on-axis maximum of the argon mass fraction in the case of the low argon content in the arc (Fig. 7, experimental data presented there are taken from [2]).

Differences in the experimental and modeled values of the plasma parameters are also due to the fact, that the side-on measurements are performed in the centers of the spacer regions and the theoretical curves are modeled with the assumptions fitting more to the channel regions.

Experiments show that the significant difference in the plasma composition in different arc regions along the arc are only visible in the case of the predominantly helium arc. There is also a possibility of visible differences in compositions between the spacer and channel regions close to the arc walls, driven by temperature gradients shown in Fig 3. Existence of these differences could perhaps be verified by performing more detailed measurements inside the spacer regions, especially close to the segment. Such measurements are yet to be performed.

Conclusions

The results show that there are many non-homogeneities in plasma composition in the multi-element plasma in the wall-stabilized arc. Significant non-homogeneities in the plasma composition along the arc are predominantly visible if the working gas contains large percentage of helium, but there is also a possibility of additional local non-homogeneities between the spacer and channel regions, especially close to the arc walls.

The non-homogeneities should be taken into account in planning and execution of the experiments in which the end-on measurement scheme is used and the plasma homogeneity along the optical axis is important. Results presented here suggest that in such a case measurements should be performed close to the arc axis (regions inside the ~ 1.2 mm radius), spacers should be as thin as possible and the percentage of helium should not be high. In the case when the percentage of helium is high, the homogeneity along the axis should be verified and the possible errors taken into account.

References

1. Bartecka A, Bacławski A, Wujec T, Musielok J (2006) Stark broadening and shift measurements of two doubly excited N I multiplets. Eur Phys J D 37:163–169
2. Książek I (2008) Experimental studies of demixing in Ar-N plasmas produced in a wall stabilized arc. Contrib Plasma Phys 48:347–356
3. Książek I, Pawelec E (2003) Study of uniformity of plasmas produced in a wall stabilized arc. Contrib Plasma Phys 43:73–77
4. Murphy AB (1997) Transport coefficients of helium and argon-helium plasmas. IEEE Trans Plasma Sci 25:809–814
5. Murphy AB (2001) Thermal plasmas in gas mixtures. J Phys D: Appl Phys 34:R151–R173
6. Musielok J, Pawelec E, Griesmann U, Wiese WL (1999) Atomic transition probabilities of FI spectral lines from 3s-3p and 3p-3d transition arrays. Phys Rev A 60:947–955
7. Pawelec E, Pokrzywka B, Delalondre C, Pellerin S, Chapelle J (2001) LTE modelisation of an argon transferred arc with orifice anode. High Temp Mater Processes 4:229–242
8. Wujec T (2005) Spectroscopic diagnostics of plasma in arc and barier discharges and measurements of atomic constants. Monography. University of Opole, Opole, pp 79–84 (in Polish)